JOURNAL OF SOLID STATE CHEMISTRY 44, 174–185 (1982)

Extended Defect Formation in Oxides with the ReO_3 Structure, I

A. N. CORMACK,* RACHEL M. JONES,†,‡ P. W. TASKER,‡
AND C. R. A. CATLOW*

‡ *Theoretical Physics Division, AERE Harwell, Didcot, Oxon OX11 ORA,
England, and * Department of Chemistry, University College,
20 Gordon Street, London WC1H OAJ, England*

Received December 30, 1981; in revised form April 20, 1982

We present results of a detailed atomistic computer simulation study of extended defect formation in ReO_3-structured nonstoichiometric oxides. Our results show, in accordance with experiment, that {102} shear planes are the most energetically favored *isolated* shear planes in such oxides. However, we show that lattice relaxations play an essential role in stabilizing these defects over {001} and higher-index planes. The latter are, however, sufficiently close in energy to permit the difference in the energies of the isolated defects to be outweighed by the defect interaction term considered in Part II of this study. We also establish that the energies of point defect modes of reduction for these oxides are sufficiently close to allow dissociation of shear planes into vacancies at very low deviations from stoichiometry.

1. Introduction

It is well established that the reduction of certain transition metal oxides (TiO_2, VO_2, MoO_3, and WO_3) leads to the formation of extended, rather than point, defects (*1–3*). Electron microscopy (*1, 2*) has demonstrated that crystallographic shear planes are present in these reduced oxides and has provided a considerable amount of structural information. The properties of these nonstoichiometric phases raise, however, a number of fundamental problems. The first concerns the factors that stabilize shear planes and the relationship between point and extended defects. Are point defects present in these oxides and if so, in what concentrations? The orientation of shear planes provides the second problem. The initial stages of reduction of WO_{3-x} lead to the formation of the {102} shear plane. With increasing deviation from stoichiometry, the {103} and then {104} planes are observed, but are replaced at the highest degree of reduction by {001} planes. These observations obviously raise the question of the relative stabilities of the different shear plane orientations, and the factors which lead to the change in stability with stoichiometry. A third point concerns the observation of ordered arrays of shear plane defects which lead to homologous series of compounds (e.g., Ti_nO_{2n-1} (*4, 5*), W_nO_{3n-p} (*6, 7*)). The exceptionally large spacings (100–150 Å) observed in nonstoichiometric crystals imply long interactions between the shear planes.

Theoretical investigations have until recently been based largely on continuum elasticity—a technique applied with success to the study of other extended defects, e.g., stacking faults and dislocations (*8*).

[†] Science Student Attachment, University of Bristol.

0022-4596/82/110174–12$02.00/0

Thus Tilley (*9*) and Iguchi and Tilley (*10. 11*) in a series of papers have attempted to calculate formation and interaction energies of shear planes in WO_{3-x}. Their approach combines empirical information on the enthalpy of reduction of WO_3 with estimates of the change in electrostatic energy on shear plane formation; continuum elasticity methods are used to calculate the strain energy of the host lattice surrounding an extended defect, and the interaction between these defects. Shear plane interactions were also investigated using continuum elasticity techniques by Stoneham and Durham (*12*).

Recently, however, shear planes have been studied by direct atomistic modeling—a method which has been applied with considerable success to point defects (*13, 14*). Calculations have succeeded in identifying the important factors stabilizing extended defects in TiO_{2-x} and have demonstrated that an equilibrium between point and extended defects exists in these oxides (*15, 16*). In the present paper we applied these methods to isolated shear planes in ReO_3-structured oxides[1] and the calculations were made for shear planes in ReO_3 itself. Although a reduced nonstoichiometric ReO_{3-x} does not form, the high symmetry of the crystal structure simplifies the detailed calculation. WO_3 has a distorted ReO_3 structure at low temperatures and MoO_3 adopts a different structure in its stoichiometric form which complicates atomistic simulation. Therefore the results from this study will provide general information on the behavior of crystals with the ReO_3 structure rather than relating specifically to WO_{3-x} or MoO_{3-x}.

We studied all three of the problems outlined above. The relationship between point and extended defects and the factors which control shear plane orientation are considered in this paper; the interactions between shear planes are treated in Part II. We give an account of the basic formalism necessary to treat shear plane stabilities and interactions. The techniques of our calculations are described below. We then present our results on the energetics of different shear plane orientations and the relative energies of point and extended defects. However, it is first necessary to clarify the structural aspects of shear plane formation since these defects cannot always be described in terms of the removal of a single plane of oxygen atoms followed by shear, as has been commonly assumed.

2. Shear Plane Structure and Oxygen Elimination

The rationalization of the complex structural geometry of crystallographic shear planes in the ReO_3 structure has been attempted previously in two different ways. The more usual view is that these extended defects are formed by the virtual elimination of a plane of anions aligned along the defect. This is done by shearing the structure (see Fig. 1). It can be seen that a necessary feature of this operation is the continuity of the anion sublattice in the defect crystal.

This idea derives from the observation that the rutile structure could be described in terms of two types of crystallographic (or lattice) planes parallel to the shear plane, one of which contained only anions, while the other contained all the cations in addition to some anions. Examination of the structure of shear planes in ReO_3-structured oxides produced an apparently similar observation: namely, that the crystallographic planes such as (102) and (103) are of two kinds, type A containing only anions, and type B containing both cations and an-

---

[1] Certain of the MoO_{3-x} shear plane systems may be included in this category, since although the stoichiometric oxide does not have an ReO_3-based structure, these reduced oxides do contain shear planes in an ReO_3-structured host.

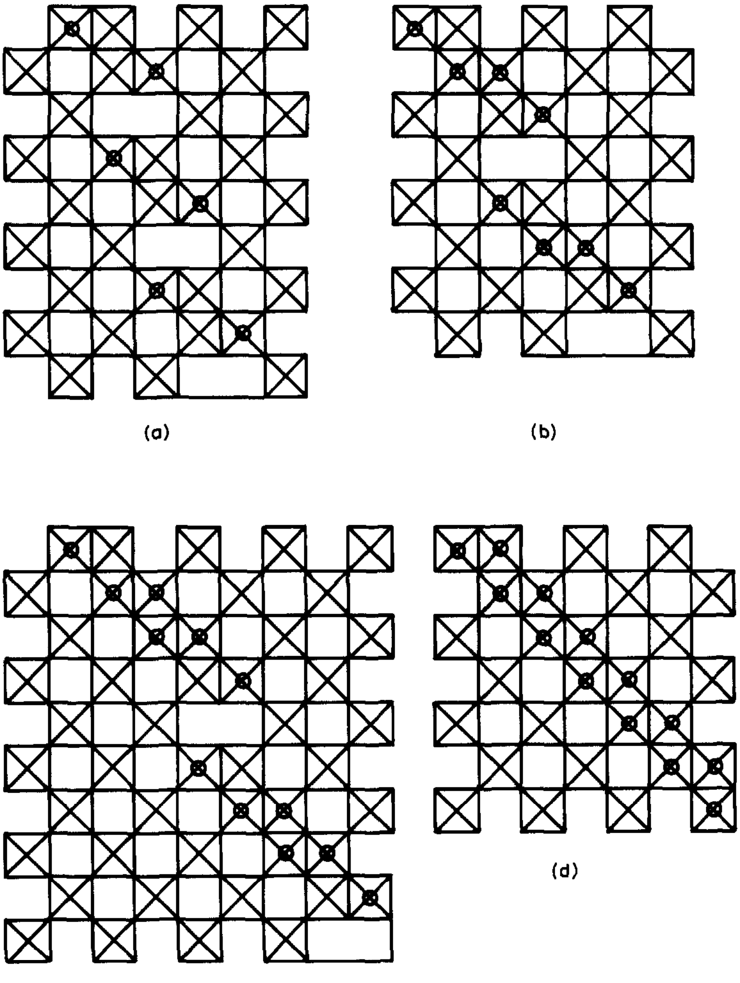

FIG. 1. Structures of the (a) (102), (b) (103), (c) (104), and (d) (001) shear planes in ReO_3-structured oxides. The diagrams show the octahedra of the oxygen sublattice with cations in the centers. The marked octahedra contain reduced cations. These positions were chosen since they give the lowest energies for the relaxed configurations.

ions. These types alternate throughout the structure to give the regular stacking sequence ABABABABAB. . . . For (102) and (103) shear planes it appears as though one plane of anions is removed to give the stacking sequence ABABBABAB. . . . In the (103) shear plane the resulting two adjacent B sheets are collapsed to form a single sheet but with twice the density of cations (see the review by Anderson (6)).

During the course of this study it became clear that this approach was not acceptable for (104) and higher-index shear planes. The simple recipe of removing a plane of anion sites and *shearing* the crystal *does not* result in a (104) shear plane since only one anion lattice site per unit cell has been eliminated. Consequently, we examined more closely the structural changes occurring during the introduction of a shear plane into the crystal.

It has already been established that in order to maintain continuity of the anion sublattice the displacement, or shear vector, which we will denote by **r** (= $\frac{1}{2}[10\bar{1}]$), must connect two anion sites. It is a common misconception that this displacement is an identity operation. Only for shear planes with odd-numbered l indices, (103), (105), etc., does the vector **r** relate anions in a plane containing only anions to identical sites in another plane. For shear planes with even l indices, (102), (104) . . . , these anions are related to anion sites in the planes containing cations. This causes all the planes of type B in the structure above the shear plane to become type A planes after the introduction of the defect plane, and vice versa.

This behavior is best understood in terms of the value of the scalar product $\mathbf{r} \cdot \mathbf{n}$, where **n** is the vector normal to the shear plane. For shear planes with odd l indices, $\mathbf{r} \cdot \mathbf{n}$ will be integral. This implies that a plane of type B is displaced onto another similar plane in going from the perfect to the defect structure. For instance, $\mathbf{r} \cdot \mathbf{n} = -1$ for (103) and so the type B plane is mapped onto the nearest type B plane on introduction of a shear plane. For (105) $\mathbf{r} \cdot \mathbf{n} = -2$ and so a plane is mapped onto the second nearest plane of the same kind, and so on. This results in the same stacking sequence of planes in the sheared structure as in the perfect structure, except that there are now type B planes with twice the den-

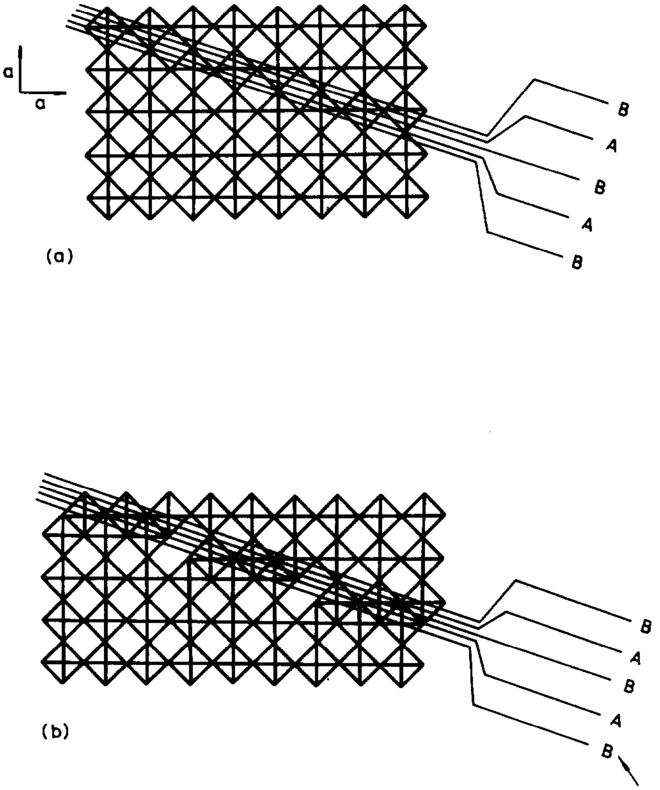

FIG. 2. (a) Unsheared ReO_3 structure showing the stacking sequence of (103) crystallographic planes. (b) Stacking sequence of (103) crystallographic planes in the sheared structure. Planes labeled A contain anions only, and those labeled B contain anions and cations. The sequence in the sheared structure is the same as in the unsheared structure except that the arrowed B plane has twice the normal density of cations.

sity of cations, the number of which is given by the absolute value of $\mathbf{r} \cdot \mathbf{n}$.

For shear planes with even l indices, (102), (104), etc., $\mathbf{r} \cdot \mathbf{n}$ will be of the form $k + \frac{1}{2}$. This implies that a type B plane will be mapped to a type A plane: the presence of the "$\frac{1}{2}$" term indicates a change in plane type after the shear operation. The value of $\mathbf{r} \cdot \mathbf{n}$ again indicates the relative displacement of the planes.

Because the type of the planes is switched, there will be a discontinuity in the stacking sequence in structures with even l-indexed shear planes. However, the number of consecutive type B (cation and anion) planes in the sequence is *not* always two. For (104) *CS* planes, this number is 4, for (106) it is 6, and in general for a (10$2l$) *CS* plane there will be $2l$ consecutive type B planes. The relationship between the stacking sequence of planes and the overall shear plane structure is illustrated for the (103) and (104) cases in Figs. 2 and 3. *Thus the deduction that shear planes are formed by annihilating a plane of anions is founded on the fortuitous examples of the (102) and (103) structures.* Rather, these extended defects involve a number of lattice or crystallographic planes which increase as the orientation of the defect changes from (102) through (103), (104), (105) . . . to (001).

The second main approach to shear plane geometry, formulated by Bursill and Hyde, resolves a lattice plane in the ReO_3 struc-

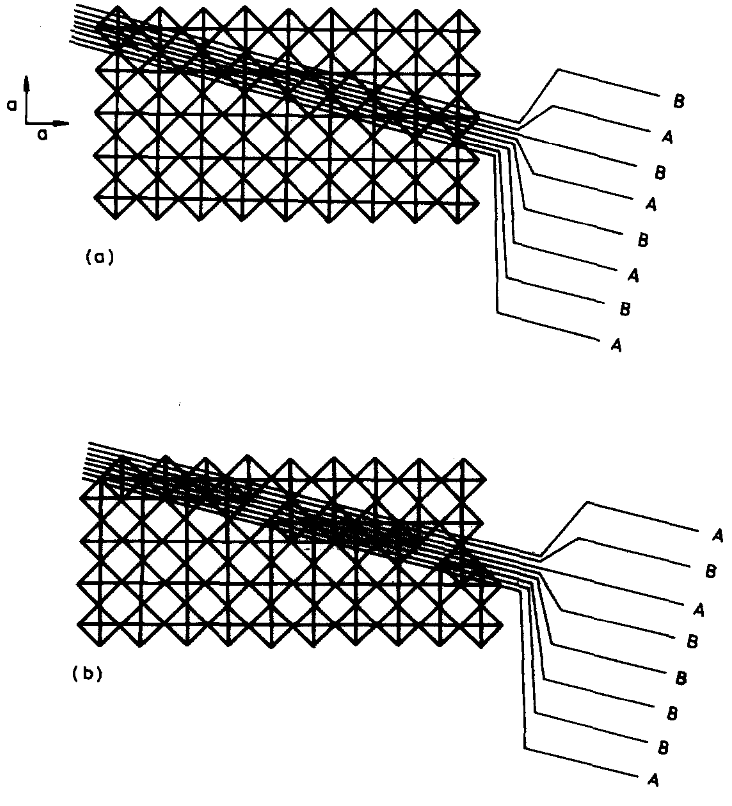

FIG. 3. (a) Unsheared structure showing regular stacking sequence of (104) crystallographic planes. (b) Stacking sequence across (104) crystallographic shear plane. The planes are labeled as in Fig. 2. The lattice planes drawn in (b) are the same as in (a) but the sequence contains four consecutive type B planes after which type A planes in the original sequence become type B planes and vice versa.

ture into two components,

$$(h0l) = p(001) + q(101)$$
$$= (q, 0, p + q),$$

where the (001) displacement produces changes in the stoichiometry and the (101) component is a conservative antiphase boundary. In the simplest case of $q = 1$, (102) shear planes are produced by $p = 1$, (103) planes by $p = 2$, etc. The number of edge-sharing pairs of octahedra in the structure is $(p + q)$ and the formulae of the various homologous series derived from regular arrays of shear planes is M_nO_{3n-p}.

This approach reinforces the conclusion of our argument since it is clear that it does not allow the formation of crystallographic shear planes to be considered simply in terms of the removal of a plane of anion lattice sites followed by collapse to restore the topology of the anion sublattice. Indeed, the displacement responsible for the nonstoichiometry of reduced ReO_3-structured oxides is always in the (001) direction when the commonly observed shear planes, (102), (103) . . . (10l), are involved.

In summary, a description of shear plane formation in terms of the elimination of planes of oxygen ions is an oversimplified approach which, although correct for certain specific cases, has no general validity. The point is crucial in theoretical studies since generation of the structures of the high-index shear planes cannot be achieved in this simple way.

3. The Energetics of Point Defect and Shear Plane Formation

Since our aim is to compare point defect and shear plane energies, and the energies of different shear plane orientations, it is necessary to express the appropriate energy terms (free energy or internal energy) in a manner which permits direct comparison between these different modes of reduction. The significant quantity to be used in such comparisons is the *energy per eliminated oxygen atom*. This is because, for a given degree of reduction, the same number of oxygen atoms must have been lost from the oxide regardless of the way in which the oxygen loss is accommodated. Thus, in thermodynamic equilibrium, the system will adopt the structure which minimizes the free energy per eliminated oxygen atom. We have neglected entropy contributions to the free energy in our calculations; this term is unlikely to be significant in the comparison of different shear plane orientations. We should emphasize that the energy per unit area (*10, 11*), although of importance when strain energy terms are concerned, is nevertheless *not* the quantity which should be used for comparisons. Energy per unit area is the important quantity when discussing the properties of conservative defects (e.g., dislocations and stacking faults); but for nonconservative defects the energy per degree of reduction or oxidation is the essential term.

We assume that reduction of the oxide to produce point defects would occur through the formation of anion vacancies[2] rather than cation interstitials. This assumption is supported by point defect calculations discussed later. Thus reduction results in the creation of anion vacancies plus electrons. The simplest description of the latter assumes localization on the metal cations. For the purposes of our calculations we described the localized species as M^{5+} ions. The calculations described below are based on this description and we assume that the reduction can be represented by the reaction

$$\text{Perfect Lattice} \rightarrow O_{VAC} + 2M^{5+} + \tfrac{1}{2}O_2(g) \quad (3.1)$$

(all symbols are defined in Table I), giving,

---

[2] We have not considered more complex species in which vacancies have trapped electrons.

TABLE I

SYMBOLS USED IN EQUATIONS (3.1)–(3.3) AND (4.2)

$\mathrm{O_{VAC}}$—	Oxygen vacancy.
M^{5+}—	Metal cation in oxidation state V.
$E_{\mathrm{O}}^{\mathrm{v}}$—	Change in internal energy (per eliminated oxygen ion) on reduction with vacancy formation.
$E_{\mathrm{O}}^{\mathrm{s}}$—	Change in internal energy (per eliminated oxygen ion) on reduction with shear plane formation.
E_{v}—	Oxygen vacancy formation energy (i.e., energy to remove an O^{2-} ion from the lattice to infinity).
E_{e}—	Energy to reduce an M^{6+} ion to the M^{5+} state.
E_{D}—	The dissociation energy of oxygen.
ΔE_{s}—	Difference between energy of reduction via formation of point defects or unrelaxed shear planes.
E_{REL}—	Relaxation energy of shear plane.
ΔE_{sv}—	Difference in energy of reduction via formation of point defects and that via formation of shear planes.
x_{v}—	Concentration of vacancy point defects.

for the energy $E_{\mathrm{O}}^{\mathrm{v}}$ of reduction per eliminated oxygen atom,

$$E_{\mathrm{O}}^{\mathrm{v}} = E_{\mathrm{v}} + 2E_{\mathrm{e}} - \tfrac{1}{2}E_{\mathrm{D}} \qquad (3.2)$$

(symbols are given in Table I). Of course interaction between the electrons and the vacancies will occur at higher deviations from stoichiometry. Such terms are omitted from Eq. (3.2), which refers therefore to the system at low deviations from stoichiometry.

For shear plane formation we use the following expression for the energy of reduction, $E_{\mathrm{O}}^{\mathrm{s}}$,

$$E_{\mathrm{O}}^{\mathrm{s}} = E_{\mathrm{O}}^{\mathrm{v}} + \Delta E_{\mathrm{s}} + E_{\mathrm{REL}}, \qquad (3.3)$$

where ΔE_{s} is the difference between the energies of the vacancy plus reduced cations and that of the rigid shear plane; the latter are the structures produced by application of the shear vectors to eliminate the vacancies without allowing ion relaxations. E_{REL} is the relaxation energy, i.e., the difference between the energy of the rigid shear plane and that of the fully equilibrated structure. All shear plane energies refer to the energy per eliminated oxygen atom and include the energy of the reduced cations. The arrangement of these reduced ions in the defect plane is discussed later.

The simulations reported below will allow us to calculate directly ΔE_{s} and E_{REL}. The important term ΔE_{sv}, representing the difference between the energies of point defect and shear plane modes of reduction, which is given by $\Delta E_{\mathrm{sv}} = \Delta E_{\mathrm{s}} + E_{\mathrm{REL}}$, may thus also be obtained. Estimates of $E_{\mathrm{O}}^{\mathrm{v}}$ and $E_{\mathrm{O}}^{\mathrm{s}}$ need values of the electron affinities of oxygen and the metal cations and the dissociation energy of oxygen in addition to lattice energy terms calculated by the simulations; these will be discussed in Part II of our study.

Equation (3.3) is, we believe, a more useful way of expressing shear plane energies for atomistic treatment than are the alternative and more complex expressions used by Iguchi and Tilley (*10, 11*), which are based on continuum descriptions. In particular, the use of Eq. (3.3) focuses attention on the very important role that lattice relaxations play in determining the relative energies of shear planes.

4. Techniques

4.1. Simulation Methods

Results using two types of atomistic simulation technique are presented in this paper. The first method simulates defects that are periodic in two dimensions and is used in obtaining shear plane energies. The second performs calculations on point defects; the vacancy energies and energies of the reduced cation were obtained using this method. They have the following features in common. First, they use the Born model for the solid to calculate the formation energies of the defects. Second, they estimate the relaxation of the lattice surrounding the defect by a procedure which divides the crystal into two regions. In the inner region adjacent to the defect the coordinates of the ions are explicitly relaxed to equilibrium. In the point defect calculations, the outer region is treated by the methods of Mott and Littleton (*17*), while rigid crystal blocks are used for the planar defects. However, in the latter case, this outer boundary is allowed to move to permit volume changes and shearing of the crystal. Detailed descriptions of both point (*13, 14*) and extended (*18*) defect simulation techniques are available elsewhere. These studies have established the quantitative reliability of the methods (*14*). Limitations on the accuracy of the calculations arise entirely from interatomic potentials used in the simulations.

4.2. Potentials

We developed a pair potential model for ReO_3. The long-range Coulomb interactions are modeled by treating both metal and oxygen ions as unpolarizable entities of integral ionic charge, i.e., Re^{6+} and O^{2-} ions. Short-range potentials are described by a simple analytical function of the Born–Mayer or Buckingham form. The parameters for the O . . . O potential were based on previous studies on transition metal oxides (*19*), but it was found necessary to vary the coefficient of the attractive part of the potential. Parameters for the metal . . . oxygen interaction were adjusted to give the best possible values for measured elastic, dielectric, and structural properties of the crystal. It is particularly important in this work that our potentials, when applied to the observed crystal structure, should give negligible residual strain, because the shear plane calculations reported subsequently are performed at constant pressure, i.e., the crystal is allowed to dilate. Thus the potentials that were obtained were fitted to give very small values for these strain terms; the parameters derived, together with the calculated perfect lattice properties, are reported in Table II.

TABLE II

PARAMETERS FOR MODEL ReO_3 POTENTIAL

Short-range potentials represented by function of form = $Ae^{-r/\rho} - Cr^{-6}$

Interaction	A	ρ	C
Re . . . O	741.39	0.4383	0.0
O . . . O	22,764.3	0.1490	17.89
Re . . . Re short-range interactions ignored			

Perfect lattice Properties

(i) Lattice parameter: 3.734 Å (fitted)

(ii) Elastic constants (dyne $cm^{-2} \times 10^{11}$) (calculated)

C_{11} : 54.15

C_{12} : C_{33} : 8.096

(iii) Static dielectric constant: 11.34 (calculated)

The potentials used are of the "rigid ion" type which neglects effects arising from electronic polarization of the ions, although *displacement* polarizability is automatically included in our treatment, via relaxation effects. Our earlier work (*15, 16*) found that displacement polarization was the major factor in stabilizing shear planes. The omission of the electronic term may affect the detailed features of the results; but it is an acceptable approximation when studying a "model" ReO_3 system as in this paper. We should note that addition of polarization greatly increases the computational demands of the calculations. We also used the full ionic charges which is, of course, a considerable oversimplification. Partial charges of ~3+ have been found (for e.g., MoO_3) in recent photoelectron studies (*20*). We believe, however, that the model is adequate for our purposes as it calculates reasonable values for the cohesive, dielectric, and elastic properties of the crystal. Several studies have shown that an accurate representation of these properties is the most important requirement of potentials used in defect simulations.

5. Results and Discussions

5.1. Shear Plane Energies

We report in Table III the calculated energies for (001), (102), (103), and (104) shear planes in ReO_3. Values are given for both unrelaxed and relaxed structures, from which we obtain the relaxation energies, E_{REL}. The unrelaxed structures were generated by shearing the structure and removing the redundant oxygen ions as described in Section 2. The reduced cations were placed at sites neighboring the shear plane. In each case a number of distributions of these ions were investigated and the results given in Table III correspond to the distributions with the lowest relaxed energies. These distributions of reduced cations are shown on Fig. 1. We should note that these configurations are not always the most favored for the unrelaxed structures. The relaxed structure for the (102) plane is illustrated in Fig. 4.

TABLE III

ENERGIES OF SHEAR PLANES IN ReO_3 PER ELIMINATED OXYGEN ION[a]

Shear plane orientation	Unrelaxed energy (eV)	Energy after relaxation (eV)	E_{REL} (eV)
{102}	181.77	128.59	53.18
{103}	166.76	129.39	37.37
{104}	161.59	129.50	32.09
{001}	152.35	129.46	22.89

[a] These energies include only the lattice energy contribution to the total shear plane energy.

The most striking feature of the results concerns the magnitudes of the relaxation energies. These are clearly a major term in the total shear plane energy and no theory which omits lattice relaxations can achieve

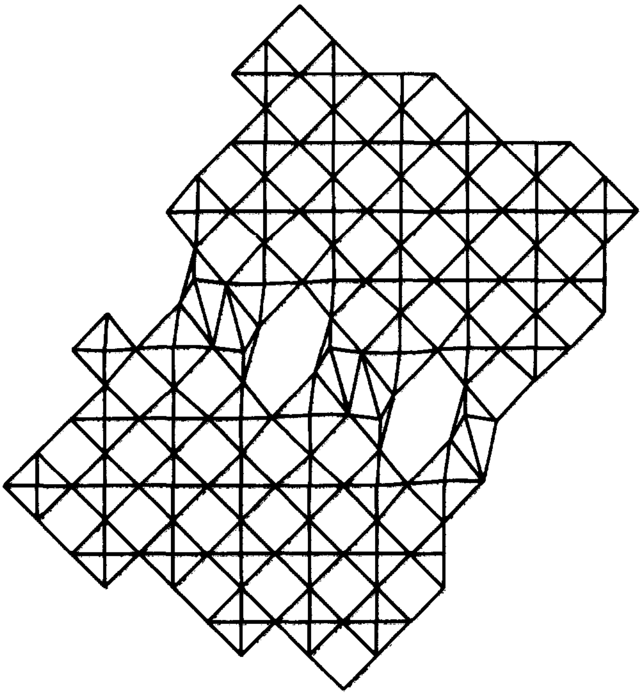

FIG. 4. This shows the distortion in the anion sublattice around a (102) shear plane from the results of the computer simulation.

results of quantitative significance. The results also underline a point we have made in previous publications (*15, 16*), namely, that lattice relaxation is a vital factor in stabilizing extended defects.

On examining the calculated unrelaxed lattice energies we find large differences of ~10–20 eV between the three types of shear plane. The predicted order of stabilities for the unrelaxed plane gives the (001) defects as most stable and the (102) as least stable. This result contrasts with the earlier calculations, using a semiempirical approach, reported by Tilley (*9*). However, Tilley's analysis, which was based on considerations of the energy per unit length of the shear plane, gives the *same* energy per eliminated oxygen for all shear plane orientations and therefore does not allow one to draw any conclusions concerning the preferred initial formation of (102) shear planes. This underlines the importance of using quantities which permit comparison between the different orientations; the energy per eliminated oxygen is, as stressed earlier, appropriate in this case.

In contrast to these marked differences between the energies of the unrelaxed planes, those of the relaxed shear planes are very similar. Moreover, *after relaxation, the (102) shear plane is found to be the most stable*. The greater stability of the (102) plane is thus entirely due to the occurrence of more extensive lattice relaxation around these defects. Relaxation is more restricted around the (001) defect, as ion displacements are constrained to be perpendicular to this plane by symmetry; the lower-symmetry (102) plane permits lateral as well as perpendicular ion relaxations. Indeed the (102) plane appears to give the maximum degree of relaxation; those obtained for the (103) and (104) defects are considerably less. These qualitative differences between the relaxations around the different shear planes have important consequences for the interactions between the defects; these effects will be explained in Part II of this study. A remarkable feature of the calculations is that despite large differences between the unrelaxed defect energies, the energies of the final relaxed configurations are very close. The similarity in the final defect energies is due to the ability of these materials to screen the interactions between defects through structural relaxation. This is, of course, the factor which is responsible for the stability of shear planes with respect to point defects and is associated with the relatively high dielectric constants. Specifically, the regions between groups of edge-sharing octahedra in the unrelaxed structures (Fig. 1) are associated with particularly high strain. Therefore the strain energy per oxygen eliminated decreases with increasing numbers of edge-sharing octahedra and hence orientation index. But the lower strain involved in these structures leads to lower relaxation energies. Indeed, the high static dielectric constant causes nearly exact compensation for the differences in unrelaxed strain. The (102) shear plane emerges with the lowest energy since the relaxation is the least constrained. The unrelaxed energies indicate the opposite order of shear plane stability.

The prediction of the (102) plane as the lowest energy structure accords with the observation of these defects in near stoichiometric WO_{3-x} (*2*). Moreover, the differences between the energies of the different shear planes are of the same order as the interaction energies between these defects, calculated in Part II. *Interactions between shear planes could therefore alter the orientations of the defects*, leading to the observed change in shear plane structure with composition. A detailed discussion of this topic will be presented in Part II of this study.

5.2. Point Defect–Shear Plane Equilibria

We have shown elsewhere (*22*) by a simple statistical mechanical argument that for systems containing shear planes, there must exist an equilibrium concentration of point defects. If vacancies are assumed to be the predominant point defect, then since a shear plane may be considered as a collapsed vacancy aggregate, the equilibrium may be represented by the following type of reaction,

$$\text{shear plane} \rightleftharpoons \mathrm{O}_{\mathrm{VAC}} + 2e^{-}, \qquad (4.1)$$

where $\mathrm{O}_{\mathrm{VAC}}$ represents the oxygen vacancy and e^{-} the electrons created on reduction. If x_{v} is the vacancy concentration, the reaction represented in Eq. (4.1) will give rise to the mass-action expression

$$K = 4x_{\mathrm{v}}^{3},$$

provided the variation of shear plane activity with concentration can be ignored. If we approximate the free energy change associated with reaction (4.1) by the internal energy term, ΔE_{sv}, as defined in Section 2, we may then write

$$4x_{\mathrm{v}}^{3} = \exp(\Delta E_{\mathrm{sv}}/kT). \qquad (4.2)$$

ΔE_{sv} for dissociation of the various shear planes depends on the energies of the isolated vacancies and reduced cations. Calculations were performed using the point defect simulation methods discussed in Section 4, and the results are reported in Table IV. The values of E_{sv} for the three shear planes are also given in Table IV. In all cases, E_{sv} is negative in accordance with the observation of extended defects in these systems. Also reported are the calculated values of ΔE_{sv}, i.e., the difference between point and extended defect energies, when relaxation is omitted from the latter. The large positive values once again emphasize the importance of lattice relaxation in stabilizing the extended defects.

TABLE IV

Point defect formation energies	
Anion vacancy	17.54 eV
Re^{5+} cations	56.59 eV

Energy, ΔE_{sv} of vacancy relative to point defects

Shear plane orientation	ΔE_{sv} (eV)	ΔE_{s} (eV)	x_{v}[a]
{102}	−2.13	51.05	0.2×10^{-3}
{103}	−1.33	36.05	3.7×10^{-3}
{104}	−1.22	31.17	5.6×10^{-3}
{101}	−1.26	21.63	4.8×10^{-3}

[a] This calculation refers to 1000K.

The values of x_{v} for a temperature of 1000K are reported in Table IV. In all cases we predict *appreciable concentrations of vacancies in equilibrium with the shear planes* at these temperatures. Shear plane dissociation into vacancies will be complete for compositions with a deviation from stoichiometry, less than x_{v}. Our results predict, therefore, that there will be a significant range of compositions in the near stoichiometric region for which point defects dominate. Tilley (*23*) has shown that for $\mathrm{WO}_{2.994}$ in the temperature range 1000–1500K, shear planes are still present. This composition is close to the boundary between the formation of shear planes and point defect disorder predicted by our calculations. It would be interesting to determine whether extended defect dissociation, as suggested by our results, was indeed observed in the nearer stoichiometric region.

An additional possibility is the dissociation of extended defect in the *grossly* nonstoichiometric region of the phase. Repulsive defect interactions at these compositions will raise the shear plane energy and hence lower the value of ΔE_{sv}. We will return to this point in the light of our calculations of the shear plane interaction functions presented in Part II.

Finally, we return to the question of the validity of our model for the point defect structure of reduced ReO_3. Calculations on the cation interstitial found that reduction with the formation of this defect was energetically less favored than reduction with vacancy formation, although the experimental evidence on this point is unclear. We also considered the question of the charge state of the reduced cation. Our results confirmed that on reduction Re(V) is preferred over Re(IV).[3] The energetic preference for Re(V) of ~1.7 eV is, however, small and could be influenced by defect interactions.

Summary and Conclusions

The calculations discussed in this paper lead to two main conclusions. The first is that the energetic preference for (102) shear planes in reduced oxides with the ReO_3 structure is a consequence of the more extensive relaxations which occur around these defects than around the (001), (103), and (104) orientations. However, the fine balance between the energies of the different relaxed shear planes suggests that shear plane orientation may be modified by relatively small terms, e.g., those arising from the defect interactions. The second conclusion is the existence of an equilibrium between point and extended defects. A significant point defect population will affect both the transport and thermodynamic properties of these oxides.

Finally, our calculations demonstrate the necessity of atomistic calculations in these systems if qualitative reliability is to be achieved. The success of this study encourages the application of the techniques to the complex problems posed by defect interaction—the main topic of Part II.

Acknowledgments

One of us (ANC) wishes to thank the SRC for provision of a research grant to support this work.

References

1. L. A. Bursill, and B. G. Hyde, *Prog. Solid State Chem.* **7**, 177 (1972).

2. R. J. D. Tilley, *in* "MTP Int. Rev. Sci. Inorganic Chemistry" (L. E. J. Roberts, Ed.) Ser. 1, Vol. 10, p. 279, Butterworths, London (1972).

3. B. E. F. Fender, *in* "MTP Int. Rev. Sci. Inorganic Chemistry" (L. E. J. Roberts, Ed.), Ser. 2, Vol. 10, p. 243, Butterworths, London (1972).

4. S. Andersson, *Acta Chem. Scand.* **14**, 1161 (1960).

5. M. Marezio, P. F. Desnier, D. B. McWhan, and J. P. Remeike, *J. Solid State Chem.* **6**, 253 (1973).

6. J. S. Anderson, *in* "Surface and Defect Properties of Solids" (M. W. Roberts and J. M. Thomas, Eds.), Vol. 1, p. 1, The Chemical Society, London (1972).

7. J. S. Anderson, and R. J. D. Tilley, *in* "Surface and Defect Properties of Solids" (M. W. Roberts and J. M. Thomas, Eds.), Vol. 3, p. 1, The Chemical Society, London (1974).

8. J. P. Hirth, and J. Lothe, "Theory of Dislocations," p. 29, McGraw-Hill, New York, (1968).

9. R. J. D. Tilley, *J. Solid State Chem.* **19**, 53 (1976).

10. E. Iguchi, and R. J. D. Tilley, *Philos. Trans. Roy. Soc. London Ser. A* **286**, 55 (1977).

11. E. Iguchi, and R. J. D. Tilley, *J. Solid State Chem.* **24**, 121 (1978); **24**, 131 (1978).

12. A. M. Stoneham, and P. J. Durham, *J. Phys. Chem. Solids* **34**, 2127 (1973).

13. A. B. Lidiard, and M. J. Norgett, *in* "Computational Solid State Physics" (F. Herman, N. W. Dalton, and T. R. Koehler, Eds.), Plenum, New York (1972).

14. C. R. A. Catlow, *J. Phys.* **41**, C6-53 (1980).

15. C. R. A. Catlow, and R. James, *Nature (London)* **272**, 603 (1978).

16. R. James, Ph.D. thesis, University of London (1979).

17. N. F. Mott, and M. J. Littleton, *Trans. Faraday Soc.* **34**, 485 (1938).

18. P. W. Tasker, and T. J. Bullough, *Philos. Mag. A* **43**, 313 (1981).

19. C. R. A. Catlow, W. C. Mackrodt, M. J. Norgett, and A. M. Stoneham, *Philos. Mag.* **35**, 177 (1977).

20. A. Manthiram, P. R. Sarode, W. H. Manhusudan, J. Gopalkrishnan, and C. N. R. Rao, *J. Phys. Chem.* **84**, 2200 (1980).

21. R. J. D. Tilley, *Nature (London)* **269**, 229 (1977).

22. C. R. A. Catlow, Proc. Int. Conf. *in* "Modulated Structures" (J. M. Cowley *et al.*, Eds.), American Institute of Physics Conf. No. 53, Academic Press, New York (1979).

23. R. J. D. Tilley, *Mater. Res. Bull.* **5**, 813 (1970).

[3] We found that the energy for the reaction $Re^{4+} + Re^{6+} \rightarrow 2Re^{5+}$ was favored by 1.72 eV. This calculation employed data on the 5th and 6th ionization potentials of rhenium as well as the lattice energy terms calculated by the simulation.